Simulating LIGO Interferometer Optics from a FFT Modeling

LIGO-G000031-00-D

Erika D'Ambrosio

- Dealing with the code
  1. Assumptions needed in the input files.
  2. Checks for the predictable cases by means of analytical functions describing the behaviour of the interferometer.
  3. Collecting documentation.

- 1. Use of the FFT code to compute how the performance is affected by real mirrors imperfections.
  2. Organization of results & classification according to the characteristics of the included mirrors.

  The program was previously intended to fix the specifications to be requested for real mirrors by studying realistic mirrors.

- Treatment of mirror data sets & strategies for extrapolating the information from the central section to the entire surface in a consistent way.

Parameter	*Value (units)*
Mirror coatings	
Loss per surface	50 ppm
ETM HR transmission	15 ppm
ITM HR transmission	0.02995
ITM AR reflectivity	600 ppm
BS reflectivity = transmission	0.499975
BS AR reflectivity	200 ppm
RM reflectivity	0.0244
Mirror radii of curvature	
ETM	7400 m
ITM	14571 m
RM	9998.65 m
Interferometer lengths	
Arm cavity	3999.01 m
Recycling cavity	9.38 m
Michelson asymmetry	0.215 m^a
RF modulation	
Resonant sideband frequency	23.9706 MHz
Resonant sideband modulation index	0.45
Input power	6.0 W
Carrier wavelength	1.064 µm

High-precision: $c = 299792458$ m/sec.

$L_{tot} = L_1 + L_2$ $L_1 = \frac{\lambda_{mod}}{2} = 6.253336546$ m. $L_2 = \frac{\lambda_{mod}}{4} = 3.126668273$

Perfect Mirrors Configuration

Standard Units		Numerical	Analytical
waist size in arm cavities		$3.510 \cdot 10^{-2}$	$3.510 \cdot 10^{-2}$
dist. waist-ITM		973.350	973.349
spot size	RM	$3.637 \cdot 10^{-2}$	$3.640 \cdot 10^{-2}$
	ETM on	$4.5655 \cdot 10^{-2}$	$4.5655 \cdot 10^{-2}$
	ETM off	$4.5652 \cdot 10^{-2}$	$4.5655 \cdot 10^{-2}$
	BS	$3.635 \cdot 10^{-2}$	$3.637 \cdot 10^{-2}$
beam curv. rad. (BS)		10032.7	10033.5
$G_{r.c.}$		66.975	68.913
Output Power		0.947	0.999

Runs Number	Carrier Run	Sidebands Run
Iterations	869	1062
Φ_{error} RM	0.00	$-3 \cdot 10^{-4}$
Φ_{error} ITM	$-3 \cdot 10^{-15}$	$-4 \cdot 10^{-4}$

FFT Numerical Simulation

1. Electric fields distribution functions

$$E^{(2)}(s_2) \sim \int_{MIRROR1} K(s_2, s_1) E^{(1)}(s_1) dS$$

$$s_1 = (x_1, y_1) \quad s_2 = (x_2, y_2)$$

$$\begin{aligned} K(s_2, s_1) &= K(\sqrt{(x_1 - x_2)^2 + (y_1 - y_2)^2 + d^2}) \\ &\simeq K(d + \frac{(x_1 - x_2)^2}{2d} + \frac{(y_1 - y_2)^2}{2d}) \end{aligned}$$

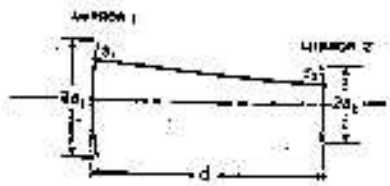

2. Steady-state resonator modes (low-order)

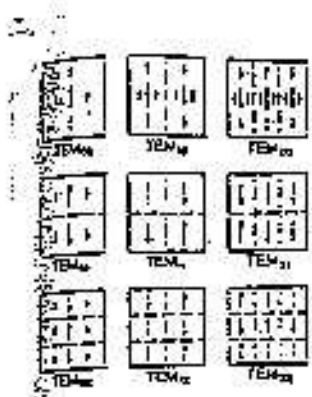

In the last three slides I showed you

the input

the core

the output

and now I will go through some boring details which are necessary to check the the right functioning of the FFT-code.

I planned a program which prompts for the same input values needed by the code and gives the same output informations but analytically evaluated.

This was for me a lovely way of learning about the beauties of optics and resonators.

Optical and Dimensional Specifications for a Fabry-Perot Cavity

- Trasmitted over Injected Power

$$\frac{I_t}{I_{in}} = \frac{(1-\sqrt{RR'})^2 - (\sqrt{R}-\sqrt{R'})^2}{(1-\sqrt{RR'})^2 + 4\sqrt{RR'}\sin^2\frac{\phi}{2}} \qquad \phi = 2L\frac{2\pi\nu}{c}$$

- Resonance Frequencies

$$\frac{\phi}{2} = n\pi \rightarrow \frac{2\pi\nu L}{c} = n\pi$$

$$\nu\triangle L + L\triangle\nu = 0 \rightarrow \frac{\Delta\nu}{\nu} = -\frac{\Delta L}{L}$$

- Free Spectral Range

$$\nu_{n+1} - \nu_n = \frac{c}{2L}$$

- Width of the Frequency Band $2\Delta\phi$

$$(1-\sqrt{RR'})^2 = 4\sqrt{RR'}\sin^2\frac{\phi}{2}$$

$$\sin^2\frac{\phi}{2} \sim (\frac{\Delta\phi}{2})^2$$

Transmitted over Injected Power if R=R'

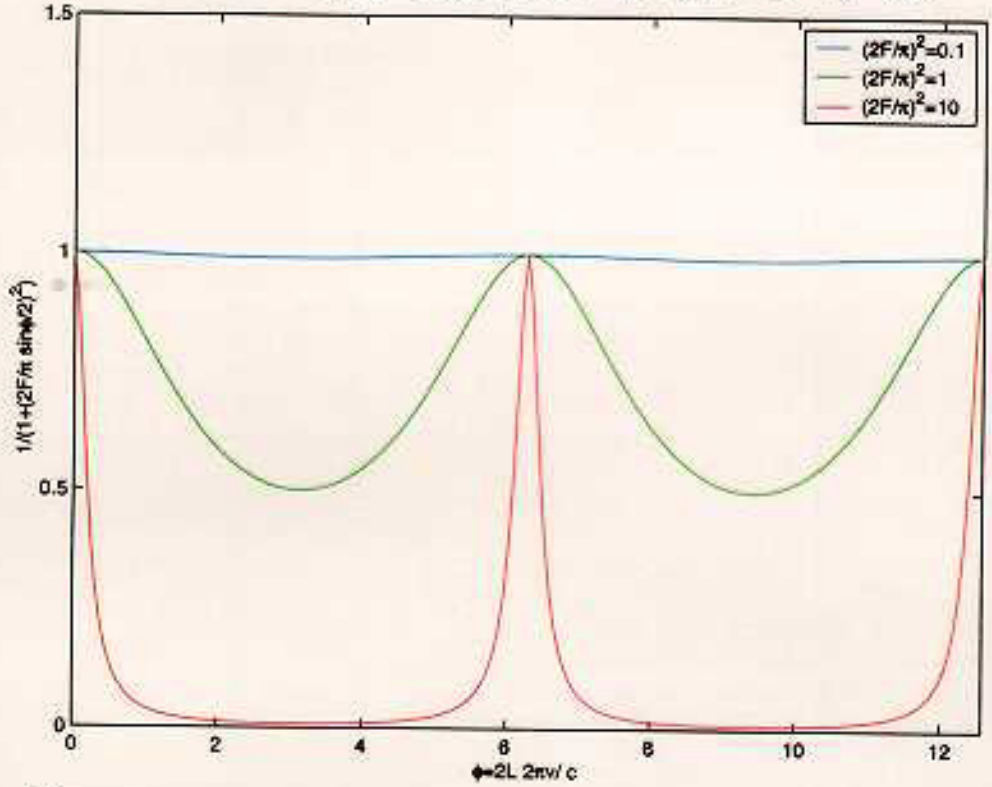

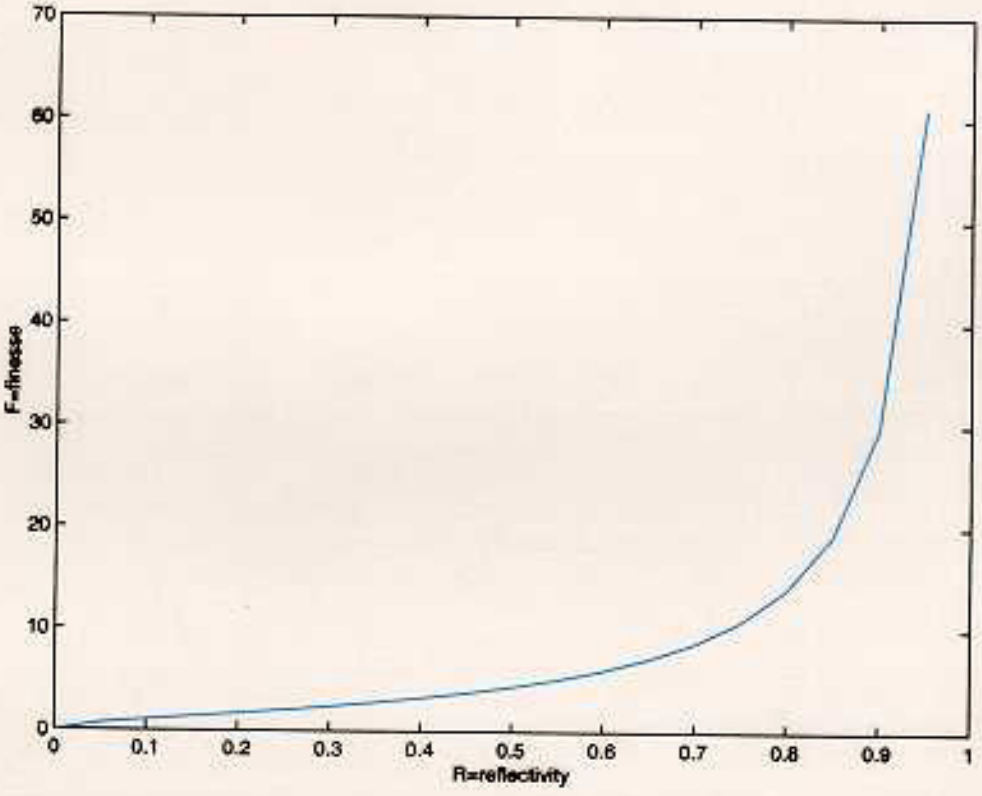

	Recycling Cavity	Long Arm Cavity
I_t/I_{in}	1	$1.3 \cdot 10^{-3}$
Bandwidth	$145KHz$	$0.181KHz$
F.S.R.	$1.5 \cdot 10^{7}Hz$	$37.5KHz$

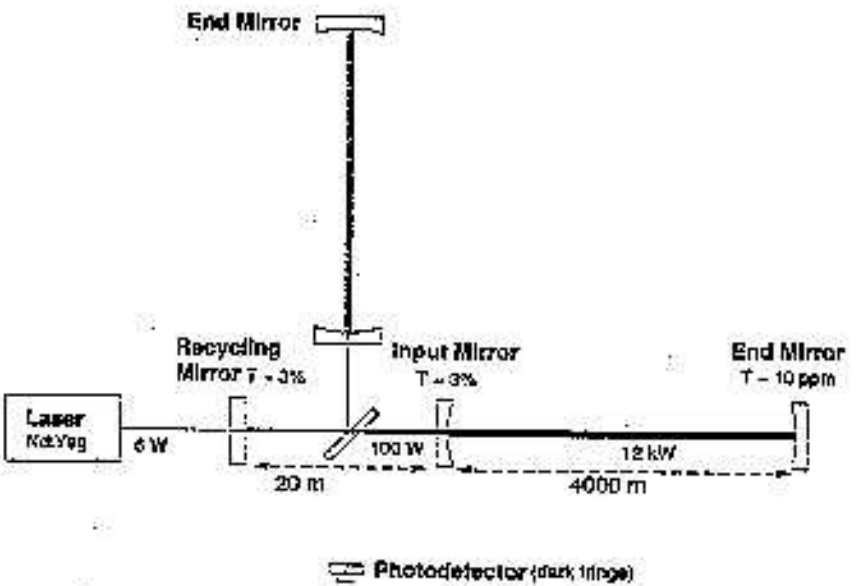

- Stored over Injected Power

$$\frac{I_{st}}{I_{in}} = \frac{T}{(1-\sqrt{RR'})^2 + 4\sqrt{RR'}\sin^2\frac{\phi}{2}} = \frac{1}{T'}\frac{I_t}{I_{in}}$$

- Reflected over Injected Power

$$\frac{I_{refl}}{I_{in}} = \frac{(\sqrt{R}-\sqrt{R'})^2 + 4\sqrt{RR'}\sin^2\frac{\phi}{2}}{(1-\sqrt{RR'})^2 + 4\sqrt{RR'}\sin^2\frac{\phi}{2}}$$

For the typical values $T = 0.03$ and $T' = 10^{-5}$

$$\frac{I_{st}}{I_{in}} = 131.2$$

$$\frac{I_{refl}}{I_{in}} = 0.9987$$

but specifying the parameter $L' = 5 \cdot 10^{-5}$ for the ETM

$$\frac{I_{st}}{I_{in}} = 130.8$$

$$\frac{I_{refl}}{I_{in}} = 0.9922$$

where the latter power ratio is equivalent to a R_{arm}.

The sensitivity of the power storage performance of the cavities to the losses in the interferometer may be figured specifying L' for the end test mass ETM.

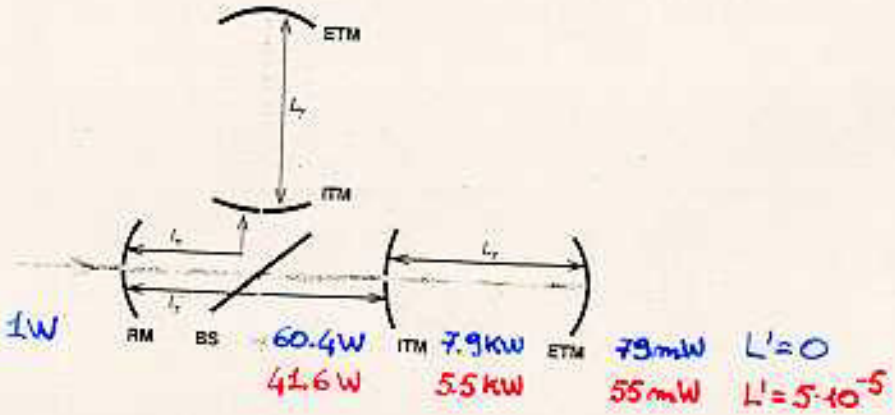

Specifications derived on the basis of resonances considerations

$$\frac{u_{ref}}{u_{in}} = -r_1 \sim -1$$

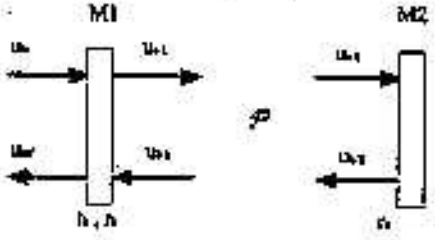

$$\frac{u_{ref}}{u_{in}} = \frac{-r_1 + r_2 e^{i\phi}}{1 - r_1 r_2 e^{i\phi}}$$

$$= \frac{-r_1 - r_2}{1 + r_1 r_2} \sim -1 \quad \phi = (2n+1)\pi$$

$$= \frac{r_2 - r_1}{1 - r_1 r_2} = \frac{1 - \sqrt{1 - t_1^2}}{1 - \sqrt{1 - t_1^2}} \sim \frac{1 - (1 - t_1^2/2)}{1 - (1 - t_1^2/2)} \sim 1 \quad \phi = 2n\pi$$

$$\phi = \frac{2\pi\nu}{c} 2L = 2n\pi \quad \phi_{sb} = \frac{2\pi(\nu \pm \nu_{mod})}{c} 2L = (2m+1)\pi$$

$$\frac{2\pi\nu_{mod}}{c} 2L = (2k+1)\pi \rightarrow \frac{2L\nu_{mod}}{c} = k + \frac{1}{2} = 639.500$$

Review of the corresponding specifications for the recycling cavity

$$\frac{2\pi\nu}{c}2L_{r.c.} = 2n\pi \qquad \frac{2\pi(\nu \pm \nu_{mod})}{c}2L_{r.c.} = (2m+1)\pi$$

$$\frac{2\pi\nu_{mod}}{c}2L_{r.c.} = (2k+1)\pi \rightarrow \frac{2L_{r.c.}\nu_{mod}}{c} = k+\frac{1}{2} = 1.50000$$

Using the notation of the FFT code

$$2kL = 2n\pi$$

is the resonance condition in the arm cavities and

$$2kL_{r.c.} = (2n+1)\pi$$

is the resonance condition in the recycling cavity if the optical cavities are considered separately.

Mode parameters of interest for a resonator with mirrors of unequal curvature

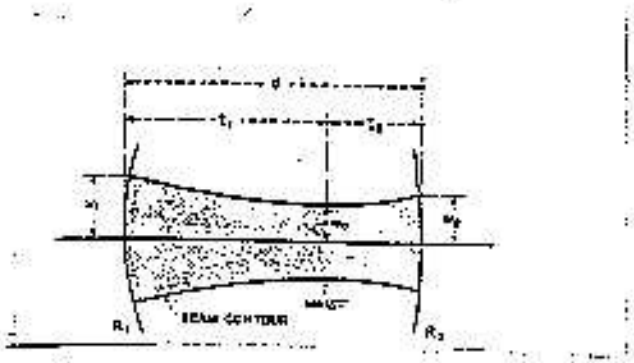

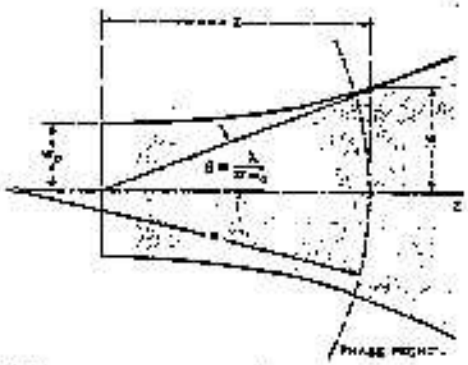

$$R_1 = 14.2km \qquad R_2 = 7.4km \qquad d = 4km$$

$$g_1 = 1 - \frac{d}{R_1} = 0.72 \qquad g_2 = 1 - \frac{d}{R_2} = 0.46$$

$$w_1 = (\frac{\lambda d}{\pi})^{\frac{1}{2}}(\frac{g_2}{g_1(1-g_1g_2)})^{\frac{1}{4}} = 3.6cm$$

$$w_2 = (\frac{\lambda d}{\pi})^{\frac{1}{2}}(\frac{g_1}{g_2(1-g_1g_2)})^{\frac{1}{4}} = 4.5cm$$

$$\nu_{qmn} = \frac{c}{2d}(q + \frac{1}{\pi}(m+n+1)\arccos\sqrt{g_1g_2})$$

The frequency spacing between TEM_{00} and TEM_{01} is $11.4KHz$ and may be best gauged by comparison with the F.S.R. which is $0.181KHz$.

Resonator Mode Configuration

$$|E_{mn}(x,y,z)| \sim \psi_n(\frac{\sqrt{2}x}{w(z)})\psi_m(\frac{\sqrt{2}y}{w(z)})$$

where $\psi_n(u) = H_n(u)e^{-\frac{u^2}{2}} = \frac{d\psi_{n-1}}{du} - u\psi_{n-1}(u)$ and

$$\frac{d^2H_n}{du^2} - 2u\frac{dH_n}{du} + 2nH_n = 0$$

$$H_{n+1}e^{\frac{-u^2}{2}} = (\frac{d}{du} - u)H_ne^{-\frac{u^2}{2}} \rightarrow H_{n+1} = \frac{dH_n}{du} - 2uH_n$$

Th. $\quad \frac{d^2H_{n+1}}{du^2} - 2u\frac{dH_{n+1}}{du} + 2(n+1)H_{n+1} = 0$

Hp. $\begin{cases} \frac{dH_{n+1}}{du} = \frac{d^2H_n}{du} - 2u\frac{dH_n}{du} - 2H_n = -2(n+1)H_n \\ \frac{d^2H_{n+1}}{du^2} = -2(n+1)\frac{dH_n}{du} \end{cases}$

and substituting

$$-2(n+1)\frac{dH_n}{du} + 4u(n+1)H_n + 2(n+1)(\frac{dH_n}{du} - 2uH_n) = 0$$

Application to Taylor's expansion:

$$\psi_n(u+\epsilon) = \psi_n(u) + \frac{d\psi_n}{du}\epsilon = \psi_n(u) + [\psi_{n+1}(u) + u\psi_n(u)]\epsilon$$

$$H_n(u+\epsilon) = H_n(u) + \frac{dH_n}{du}\epsilon = H_n(u) + [H_{n+1}(u) + 2uH_n(u)]\epsilon$$

Outline of the G.W. detection

$$E_{PD} \sim \frac{1}{2}[R_{arm}(\phi_1)e^{-i\varphi_1} - R_{arm}(\phi_2)e^{-i\varphi_2}] = 0$$

recalling that $\phi = 2kL = 2n\pi$ and $\varphi = 2kL_{r.c.} = 2m\pi$,

$$R_{arm}(\phi) = \frac{\sqrt{R} - \sqrt{R'}e^{-i\phi}}{1 - \sqrt{RR'}e^{-i\phi}} \qquad G_{r.c.} \doteq \frac{\sqrt{T_{RM}}}{1 - \sqrt{R_{RM}R_{arm}(2n\pi)}}$$

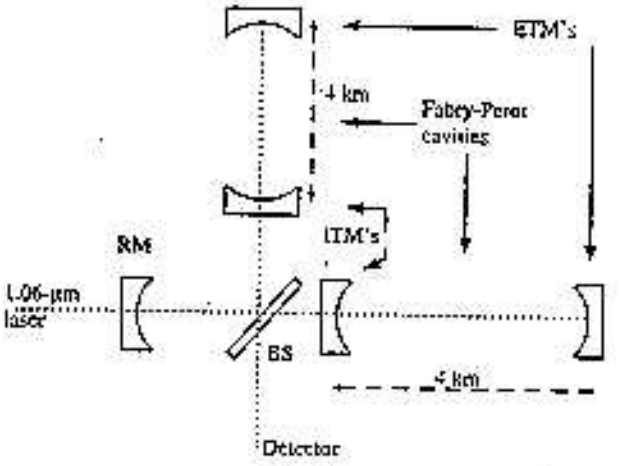

$$\phi = 2kl \pm \Phi_{gw} \rightarrow E_{PD} \sim \frac{1}{2}[\frac{\sqrt{R} - \sqrt{R'}e^{-i\Phi_{gw}}}{1 - \sqrt{RR'}e^{-i\Phi_{gw}}} - \frac{\sqrt{R} - \sqrt{R'}e^{i\Phi_{gw}}}{1 - \sqrt{RR'}e^{i\Phi_{gw}}}]$$

$$\sim \frac{(1-R)\sqrt{R'}\sin\Phi_{gw}}{(1-\sqrt{RR'})^2 + 4\sqrt{RR'}\sin^2\frac{\Phi_{gw}}{2}} \simeq \frac{(1-R)(\frac{R'}{R})^{\frac{1}{4}}\frac{2\pi FL}{\lambda}h(f)}{\pi(1-\sqrt{RR'})}$$

where $F = \frac{\pi(RR')^{\frac{1}{4}}}{1-\sqrt{RR'}}$.

Function of the frequency modulation

$$
\begin{aligned}
E &= E_l e^{i\Gamma \cos \omega_{mod} t} \\
&\simeq J_0(\Gamma) E_l + i J_1(\Gamma) E_l e^{i\omega_{mod} t} + i J_1(\Gamma) e^{-i\omega_{mod} t} \\
&= E_0 + E_1 e^{i\omega_{mod} t} + E_{-1} e^{-i\omega_{mod} t}
\end{aligned}
$$

$$
\begin{aligned}
P(\omega_{mod}) &= |E|^2 = |E_0|^2 + |E_1|^2 + |E_{-1}|^2 + \\
&\quad 2\Re[E_1 E_{-1}^* e^{2i\omega_{mod} t}] + 2\Re[E_0 E_{-1}^* + E_1 E_0^*) e^{i\omega_{mod} t}]
\end{aligned}
$$

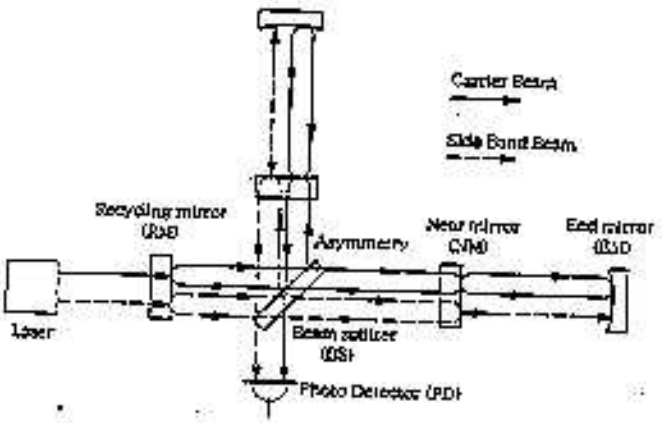

$$
\begin{aligned}
V_I &= \frac{1}{T}\int_0^T P(\omega_{mod}) \cos \omega_{mod} t dt = \Re[E_0 E_{-1}^* + E_1 E_0^*] \\
V_Q &= \frac{1}{T}\int_0^T P(\omega_{mod}) \sin \omega_{mod} t dt = -\Im[E_0 E_{-1}^* + E_1 E_0^*] \\
D.C. &= \frac{1}{T}\int_0^T P(\omega_{mod}) dt = |E_0|^2 + |E_1|^2 + |E_{-1}|^2
\end{aligned}
$$

Including Real Optical Components

Standard Units		Ideal Case	RM Real Map
waist size in arm cavities		$3.510 \cdot 10^{-2}$	$3.510 \cdot 10^{-2}$
dist. waist-ITM		973.350	973.350
spot size	RM	$3.637 \cdot 10^{-2}$	$3.637 \cdot 10^{-2}$
	ETM on	$4.5655 \cdot 10^{-2}$	$4.5655 \cdot 10^{-2}$
	ETM off	$4.5652 \cdot 10^{-2}$	$4.5652 \cdot 10^{-2}$
	BS	$3.635 \cdot 10^{-2}$	$3.635 \cdot 10^{-2}$
beam curv. rad. (BS)		10032.7	10032.7
$G_{r.c.}$		66.975	67.522
G_{arm}		4371	4406
Output Power		0.947	0.875

Runs Number	Carrier Run	Sidebands Run
Iterations	1100	803
Φ_{error} RM	0.00	$-7 \cdot 10^{-2}$
Φ_{error} ITM	$-6 \cdot 10^{-13}$	$3.6 \cdot 10^{-2}$

How all those analytical predictions are affected by using real maps ?

Putting one of the two real maps I was given so far entails no relevant change for the geometrical properties of the beam.

The power informations are a little varied and the same happens if both the RM and one of the two ITM are used for the run.

In this case again the shape of the beam remains the same but watching the power storage performances of the cavities we see that they drop down by a not negligible factor. Moreover the symmetry between the two arms is broken and the program takes a longer time to run.

By the way it stops iterations when the error on some physical quantities is less than threshold that I can fix.

Criteria for calculating the sensitivity problems of the interferometer

Shot-noise photocurrent determined by the counting

$$i_{S.N.}(f) = \sqrt{2e < I >} \quad I = \frac{\eta e \lambda}{2\pi \hbar c} P_{PD}$$

The asymmetry δ is sensed by the two sidebands

$$E_{1PD} = \frac{-i\sqrt{T_{RM}\sin\alpha}E_1}{1-\sqrt{R_{RM}}\cos\alpha} \quad E_{-1PD} = \frac{i\sqrt{T_{RM}\sin\alpha}E_{-1}}{1-\sqrt{R_{RM}}\cos\alpha}$$

$$\alpha \equiv \frac{\omega_{mod}\delta}{c}$$

Signal due to the presence of a gravitational wave

$$P_{PD} = 2E_{PD}(G_{r.c.}, \Phi_{gw})E_{1PD} = \frac{(1-R')(\sqrt{R}-\sqrt{R'})}{1-\sqrt{R_{RM}}(\frac{\sqrt{R}-\sqrt{R'}}{1-\sqrt{RR'}})} \times$$
$$\frac{4(1-R_{RM})J_1(\Gamma)J_0(\Gamma)E_l^2\sin\alpha}{(1-\sqrt{RR'})(1-\sqrt{R_{RM}}\cos\alpha)}(\frac{R'}{R})^{\frac{1}{4}}\frac{FLh(f)}{\lambda}$$
$$= \frac{2\pi\hbar c}{\eta e\lambda}\sqrt{2}i_{S.N.}(\omega_{mod} \pm f)$$

The detection is limited by:

$$h(f) = \sqrt{\frac{\hbar c\lambda}{\eta\pi P_l}}\frac{\pi(1-\sqrt{RR'})}{\sqrt{\frac{R'}{R}}FL}\frac{1-\sqrt{R_{RM}}\frac{\sqrt{R}-\sqrt{R'}}{1-\sqrt{RR'}}}{\sqrt{T_{RM}}(1-R)J_0(\Gamma)}$$
$$= 8.97 \cdot 10^{-24} \qquad \eta = 1$$

Introducing Two Measured Maps

Standard Units		Ideal Case	RM & ITM on
waist size in arm cavities		$3.510 \cdot 10^{-2}$	$3.510 \cdot 10^{-2}$
dist. waist-ITM		973.350	973.350
spot size	RM	$3.637 \cdot 10^{-2}$	$3.637 \cdot 10^{-2}$
	ETM on	$4.5655 \cdot 10^{-2}$	$4.5655 \cdot 10^{-2}$
	ETM off	$4.5652 \cdot 10^{-2}$	$4.5652 \cdot 10^{-2}$
	BS	$3.635 \cdot 10^{-2}$	$3.635 \cdot 10^{-2}$
beam curv. rad. (BS)		10032.7	10032.7
$G_{r.c.}$		66.975	62.625 −6.5%
$G_{arm\ on}$		4371	4083 −6.6%
$G_{arm\ off}$		4371	4087 −6.6%
Output Power		0.947	0.907

Runs Number	Carrier Run	Sidebands Run
Iterations	1439	815
Φ_{error} RM	0.00	$-4 \cdot 10^{-2}$
Φ_{error} ITM	$-5 \cdot 10^{-14}$	$1.1 \cdot 10^{-2}$

What the maps look like and how they must be manipulated to be used within the FFT simulation?

Size of the map

A 576×480 grid must be fitted into a 128×128

Shape of pixels

The FFT-code deals with square pixels while the measured ones are rectangular

These are two unusual problems and I did not find a standard solution in books.

I planned and algorithm of my own which is pretty flexible and I will show you an example in one dimension since the extension to the case of more dimensions is straighforward.

It can treat both the case when the informations must be distributed between a bin and another and when they all go into only one.

Moreover it gets rid of the problem of rectangular shaped pixels defining a δ_x and δ_y and I will explain you better.

ITM as measured

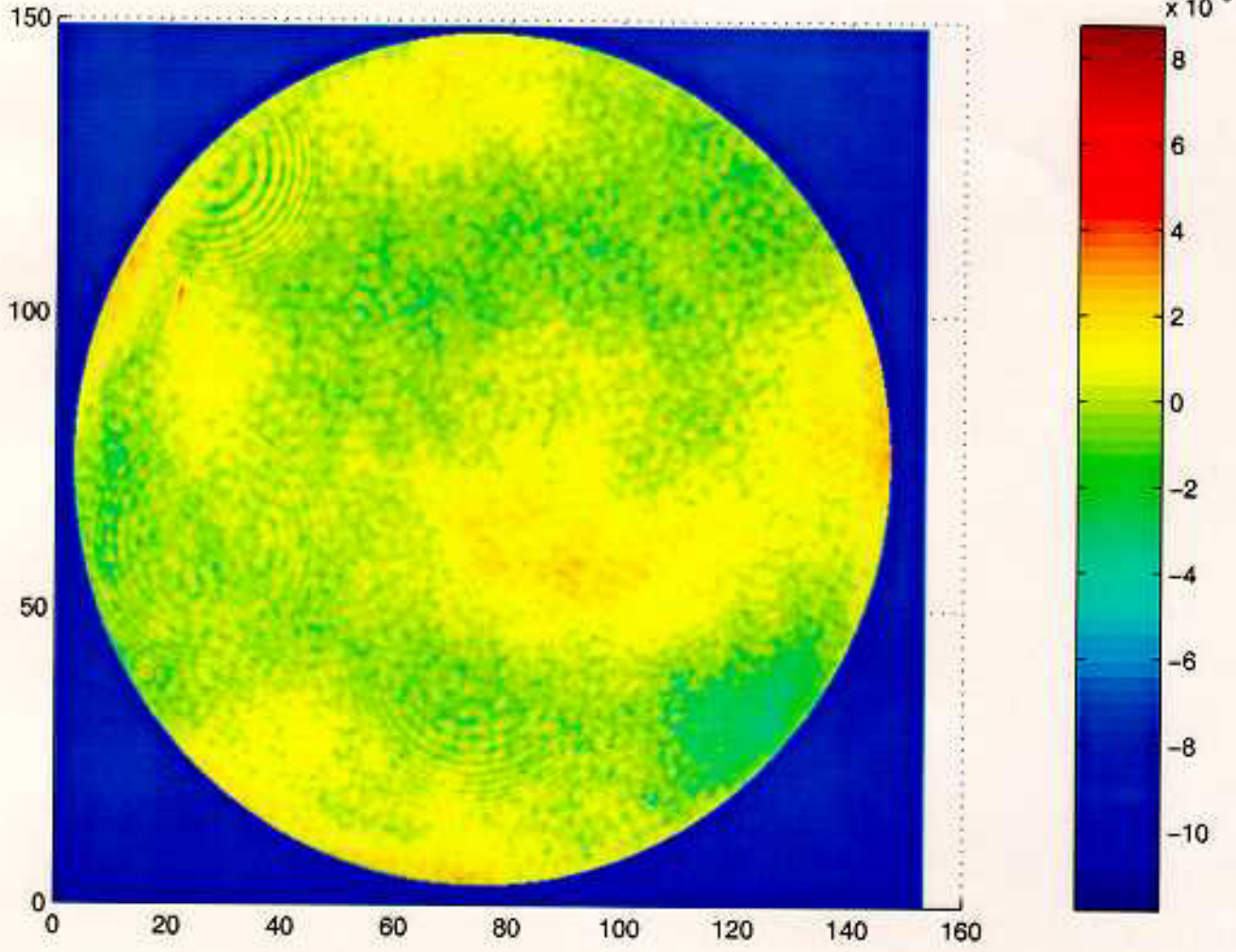

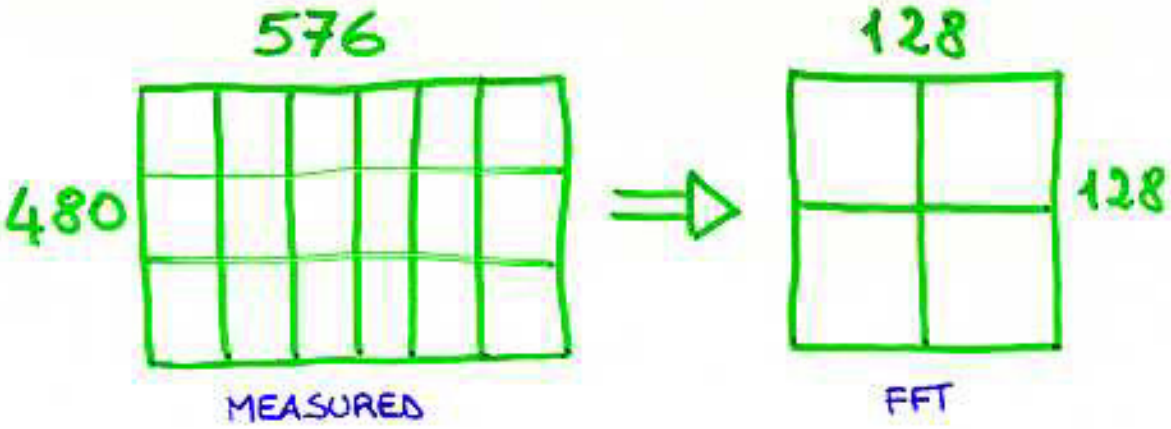

The challenge is to use all the data with uniform weights

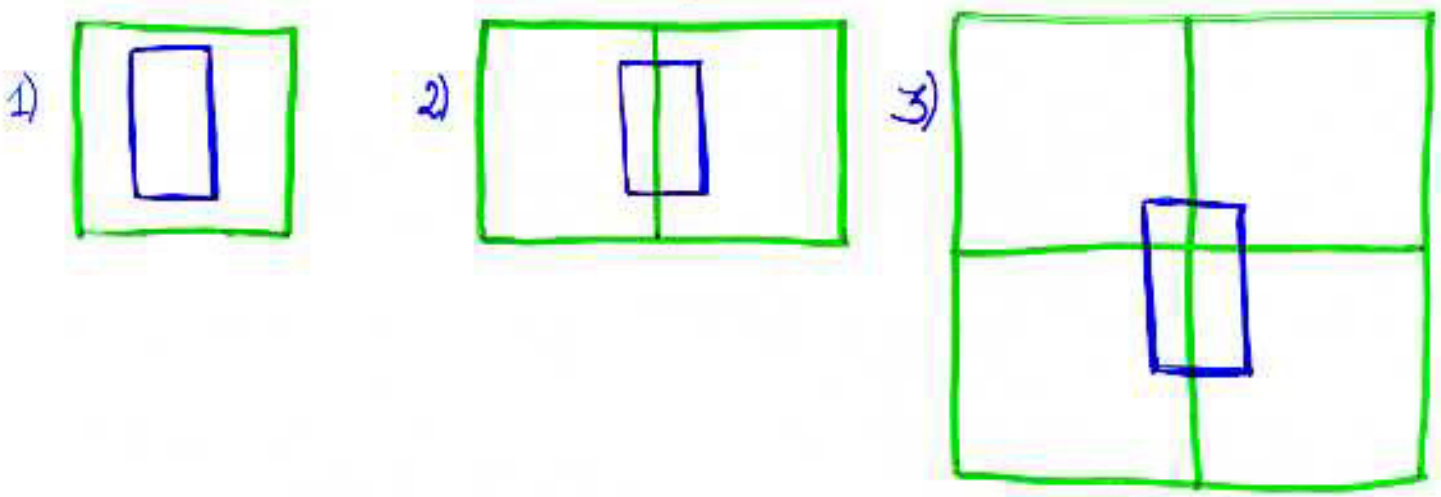

Fitting data to 128×128 regular maps with square pixels

$$(\frac{\Delta}{\delta}\text{int}[\frac{\delta(i+1)}{\Delta}] - i) \times v_1(i) \rightarrow v_2(\text{int}[\frac{\delta i}{\Delta}])$$

$$(i + 1 - \frac{\Delta}{\delta}\text{int}[\frac{\delta(i+1)}{\Delta}]) \times v_1(i) \rightarrow v_2(\text{int}[\frac{\delta(i+1)}{\Delta}])$$

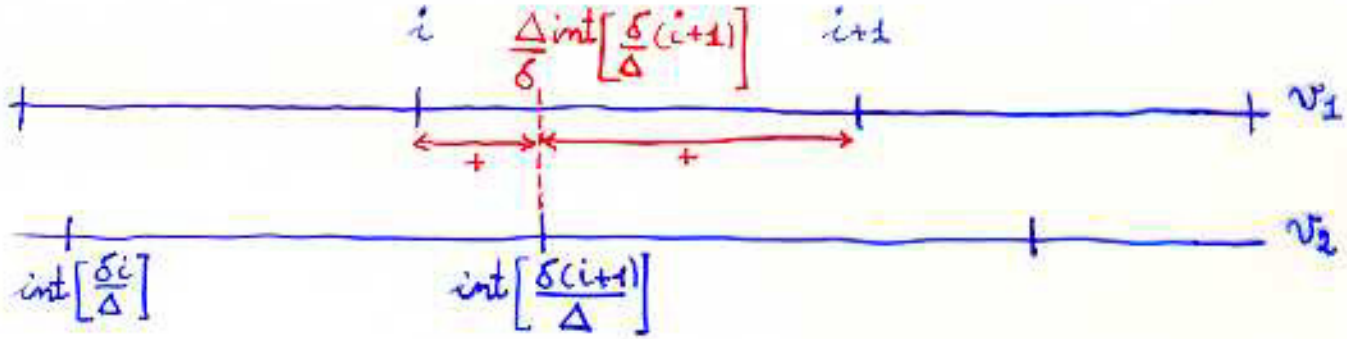

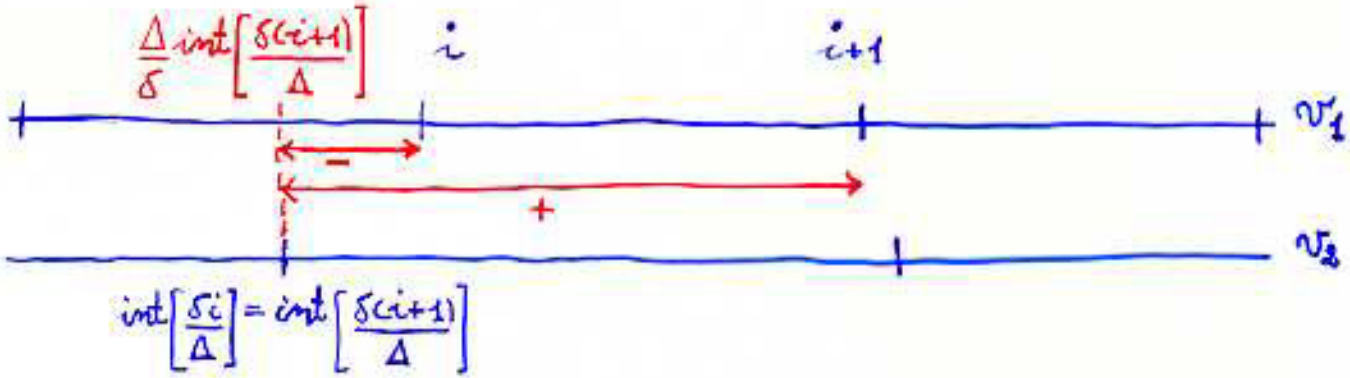

Weighted Average $\frac{\sum_i w_i v_i}{\sum_i w_i} \Rightarrow Norm = \frac{\delta}{\Delta}$

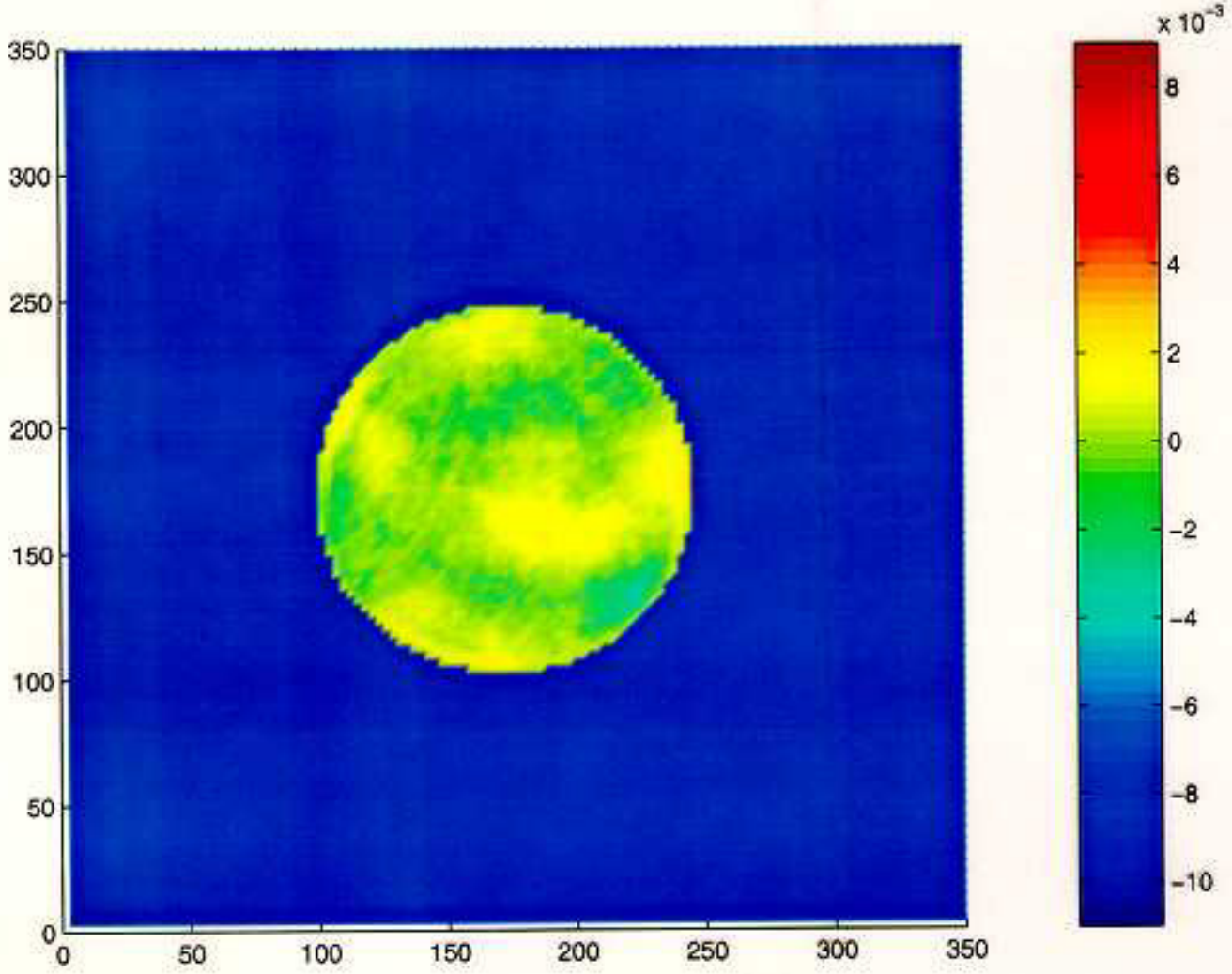

ITM as processed to match FFT-code requirements

RM as measured

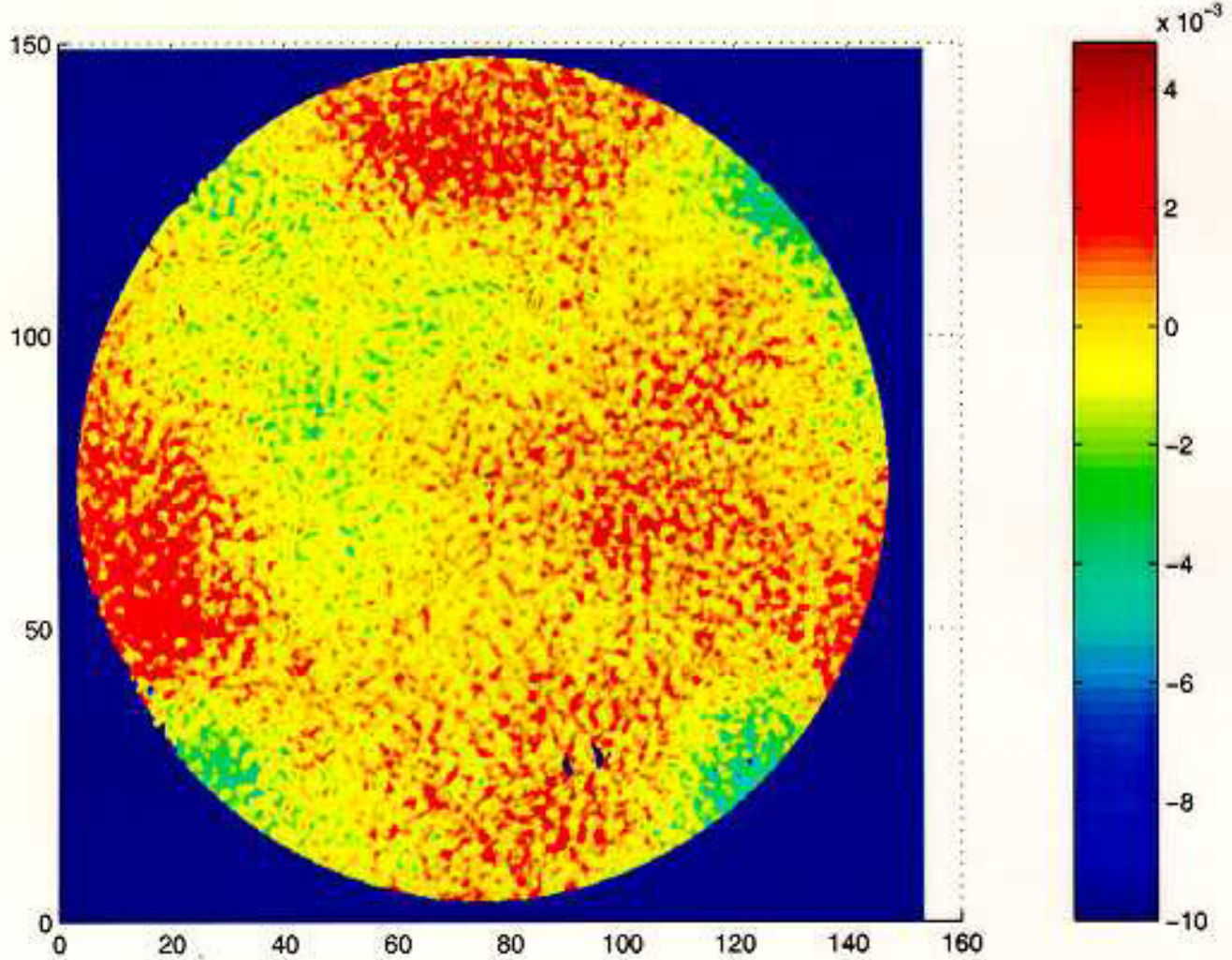

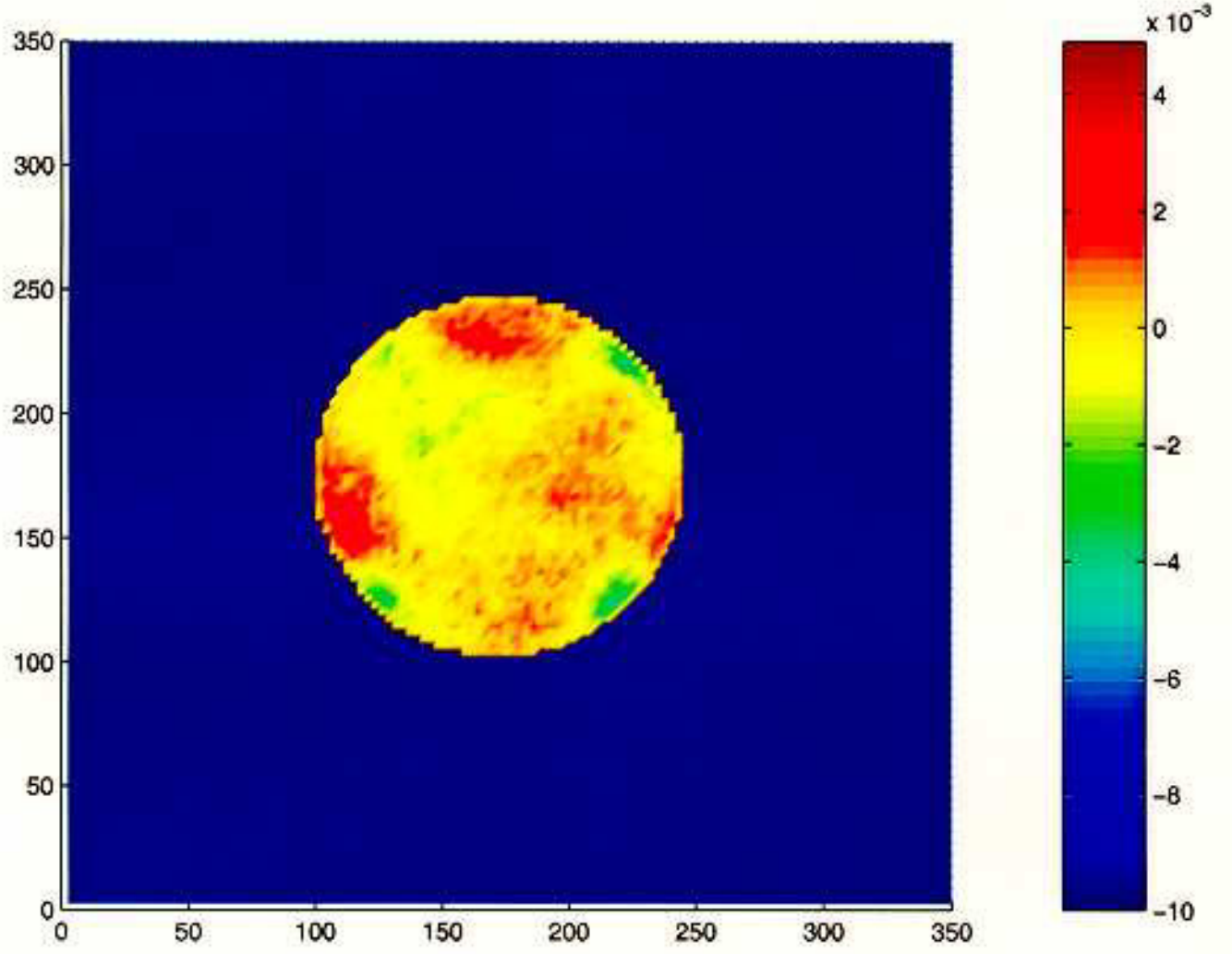

RM as processed to match FFT-code requirements

As we can see the measured and adapted maps look pretty similar but doing some statistical evaluations has given me a deeper insight.

Because of the averaging procedure the fluctuations are decreased.

What kind of informations are we losing?

Maybe some peaks have been integrated.

In the Fourier transforms space there is evidence of an effect at $3 - 3.5 cm^{-1}$.

I don't know what it is but if it is a real property of the mirror maybe related to the mechanical polishing procedure it is not taken into account by the code.

Indeed in the adapted map it is cut.

Similar high frequency peaks appear in the PSD of the RM with what appear like some harmonics.

There is no directionality as we can see from the plot.

Estimation of the first and second order statistics for the mirror maps

	The Mean Value	Standard Deviation
ITM measured	$-2.8248 \cdot 10^{-9}$	$7.3241 \cdot 10^{-4}$
ITM for FFT	$-5.1564 \cdot 10^{-10}$	$2.8994 \cdot 10^{-4}$
RM measured	$3.5518 \cdot 10^{-9}$	$9.7473 \cdot 10^{-4}$
RM for FFT	$6.5669 \cdot 10^{-10}$	$3.3947 \cdot 10^{-4}$

ITM measured

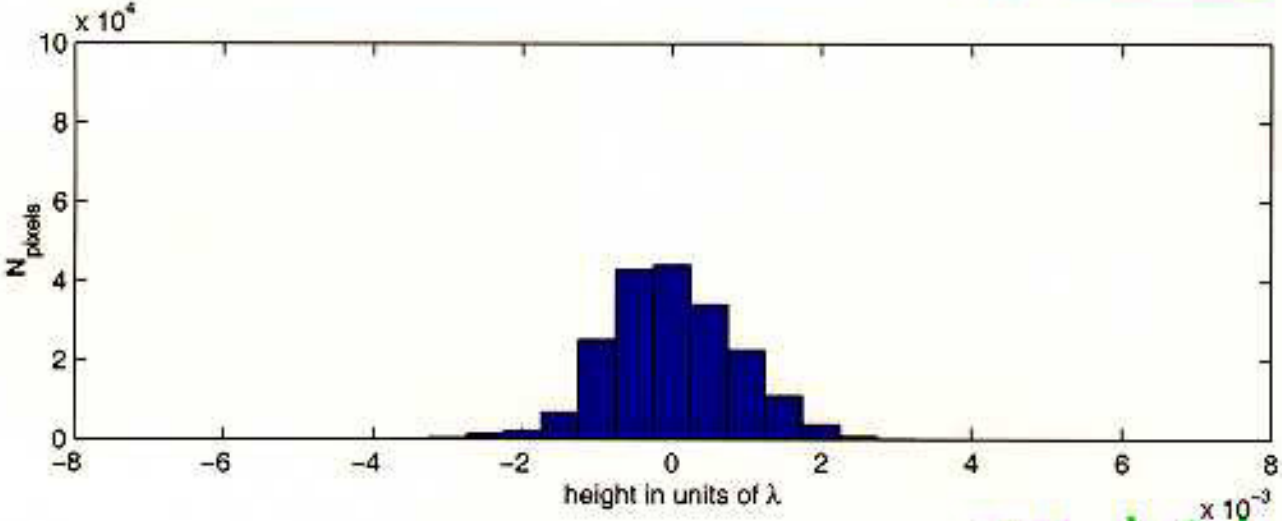

ITM adapted

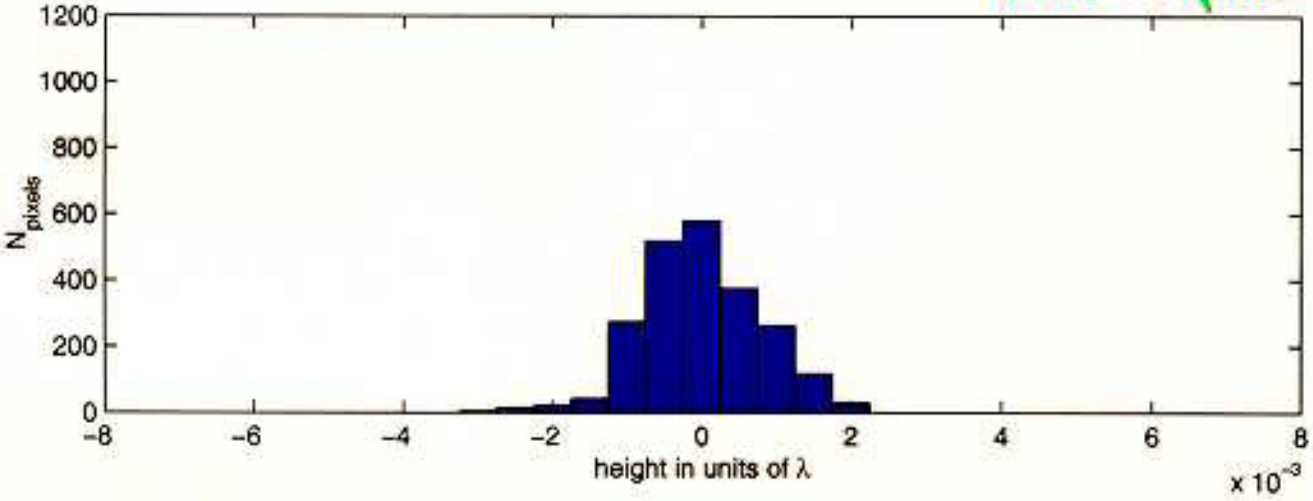

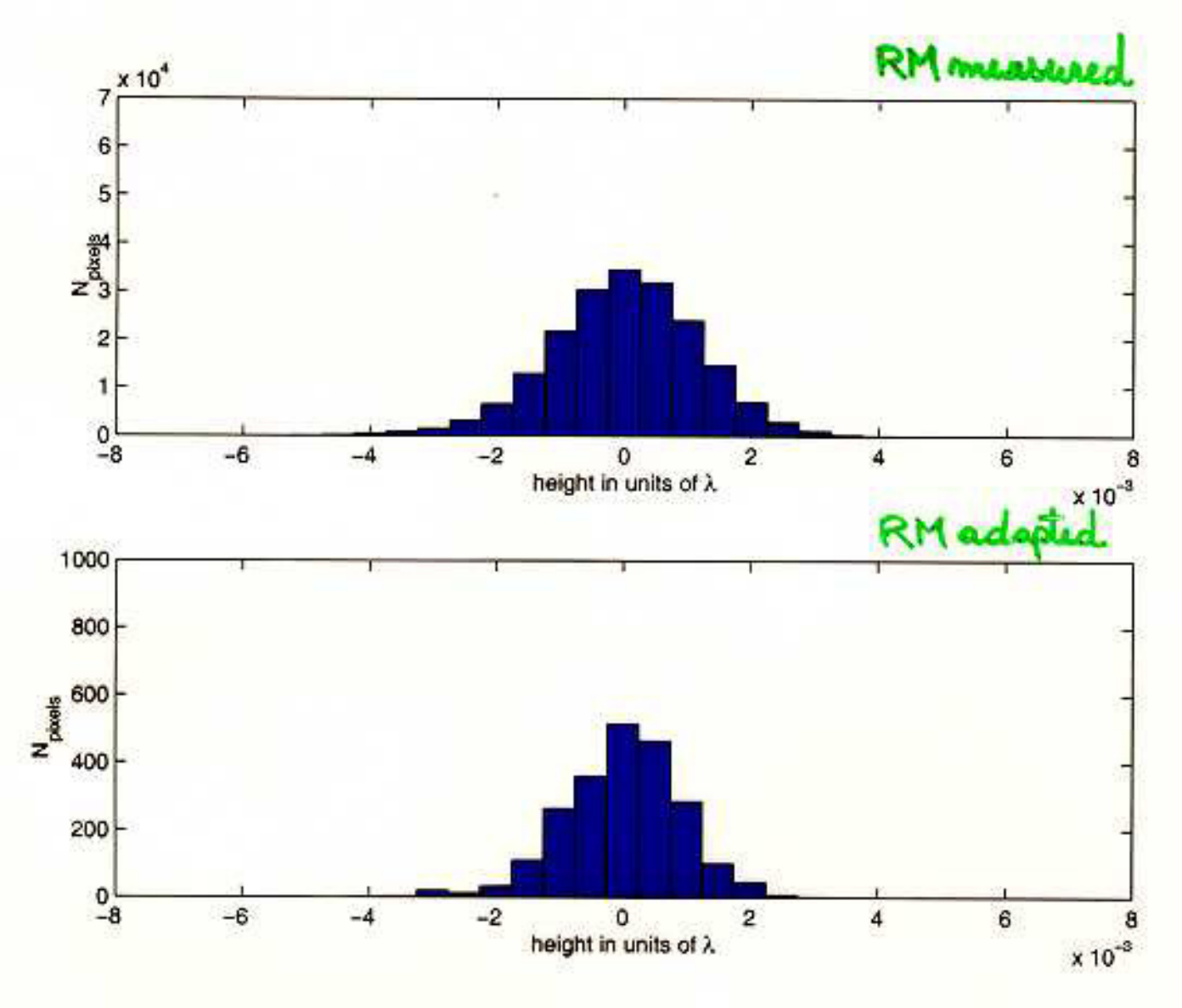
RM measured
x 10^4
7
6
5
4
3
2
1
0
N_pixels
−8
−6
−4
−2
0
2
4
6
8
height in units of λ
x 10^-3
RM adopted
1000
800
600
400
200
0
N_pixels
−8
−6
−4
−2
0
2
4
6
8
height in units of λ
x 10^-3

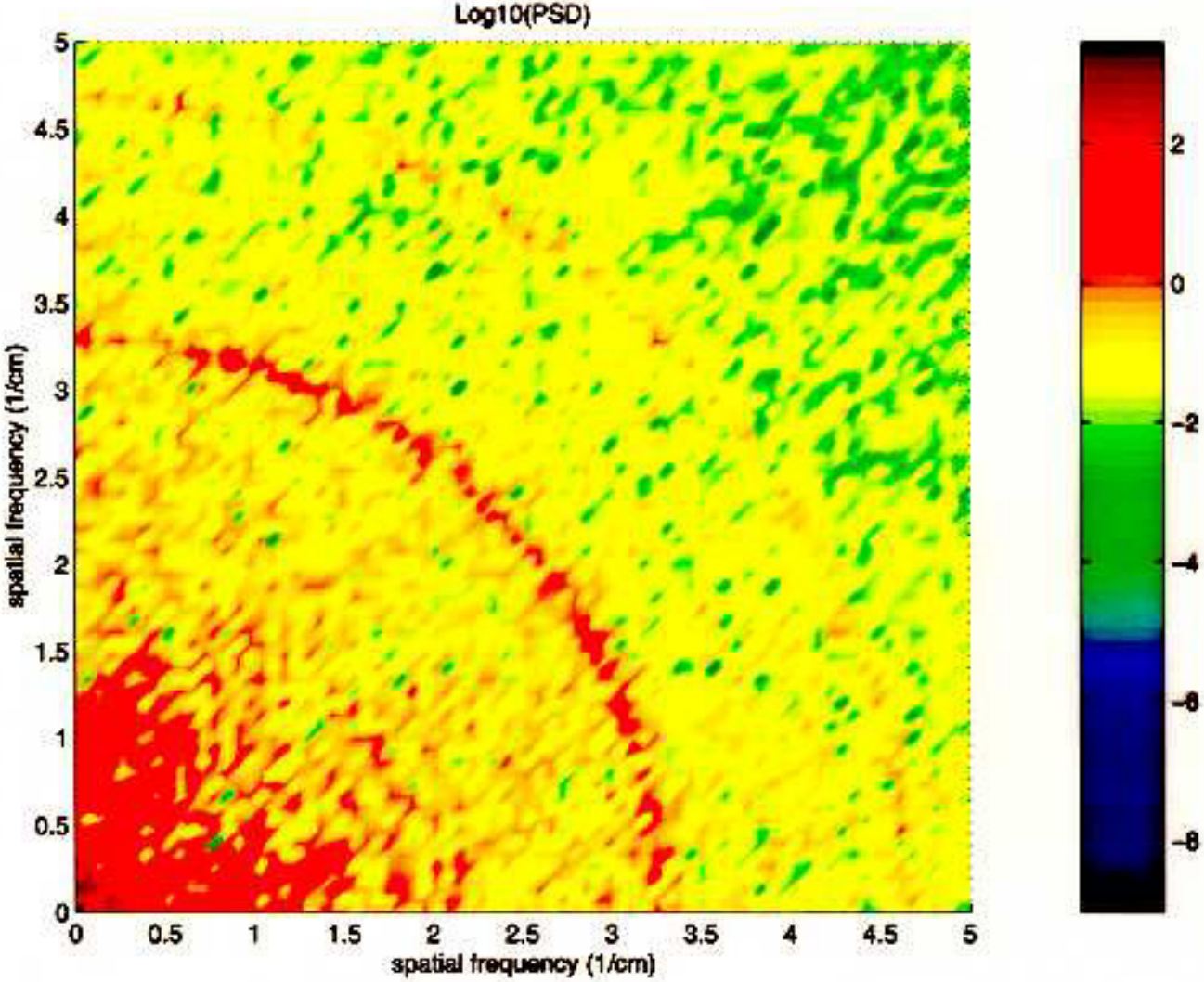
Log10(PSD)
spatial frequency (1/cm)
spatial frequency (1/cm)
0
0.5
1
1.5
2
2.5
3
3.5
4
4.5
5
2
0
-2
-4
-6
-8

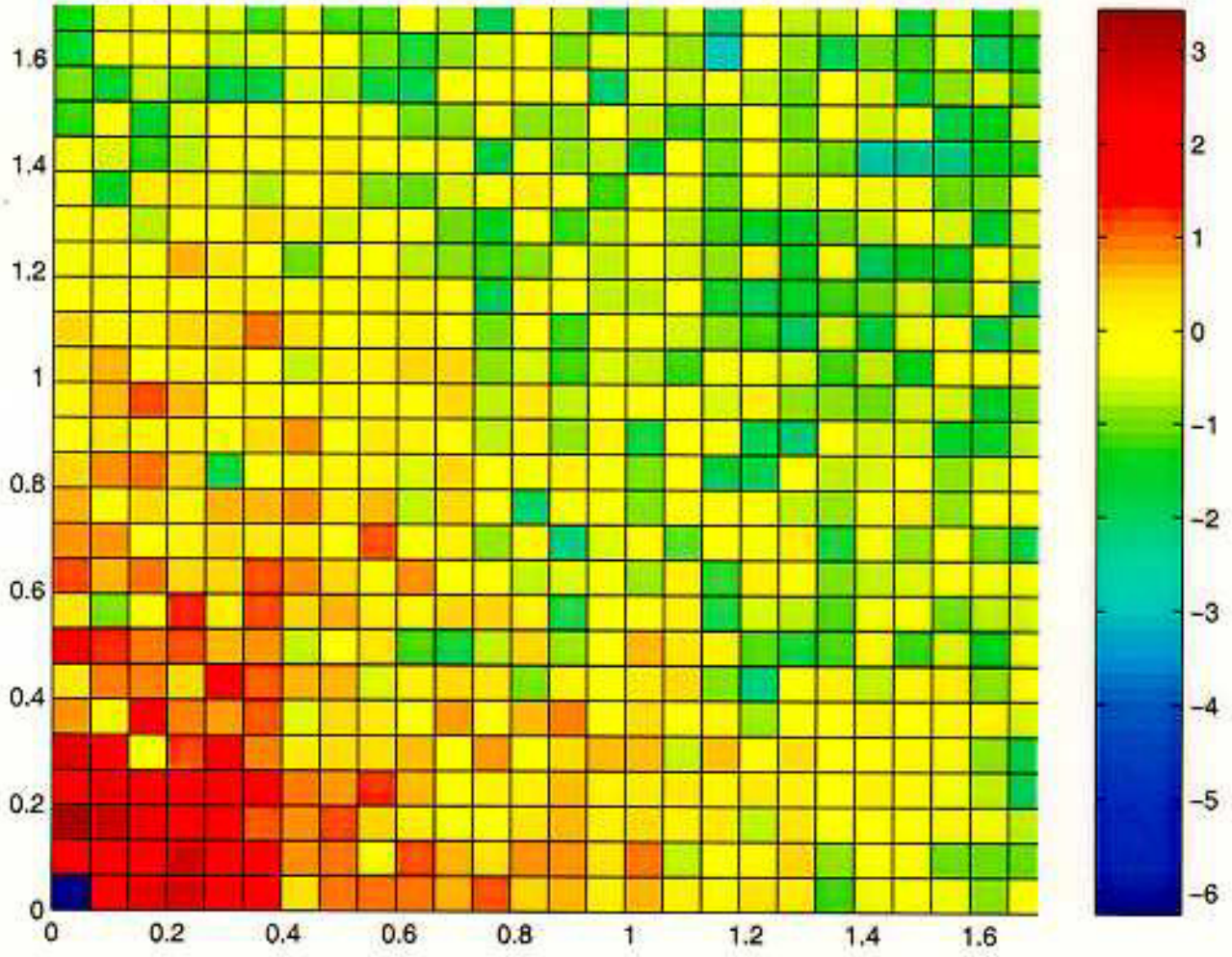
1.6
1.4
1.2
1
0.8
0.6
0.4
0.2
0
0
0.2
0.4
0.6
0.8
1
1.2
1.4
1.6
3
2
1
0
−1
−2
−3
−4
−5
−6

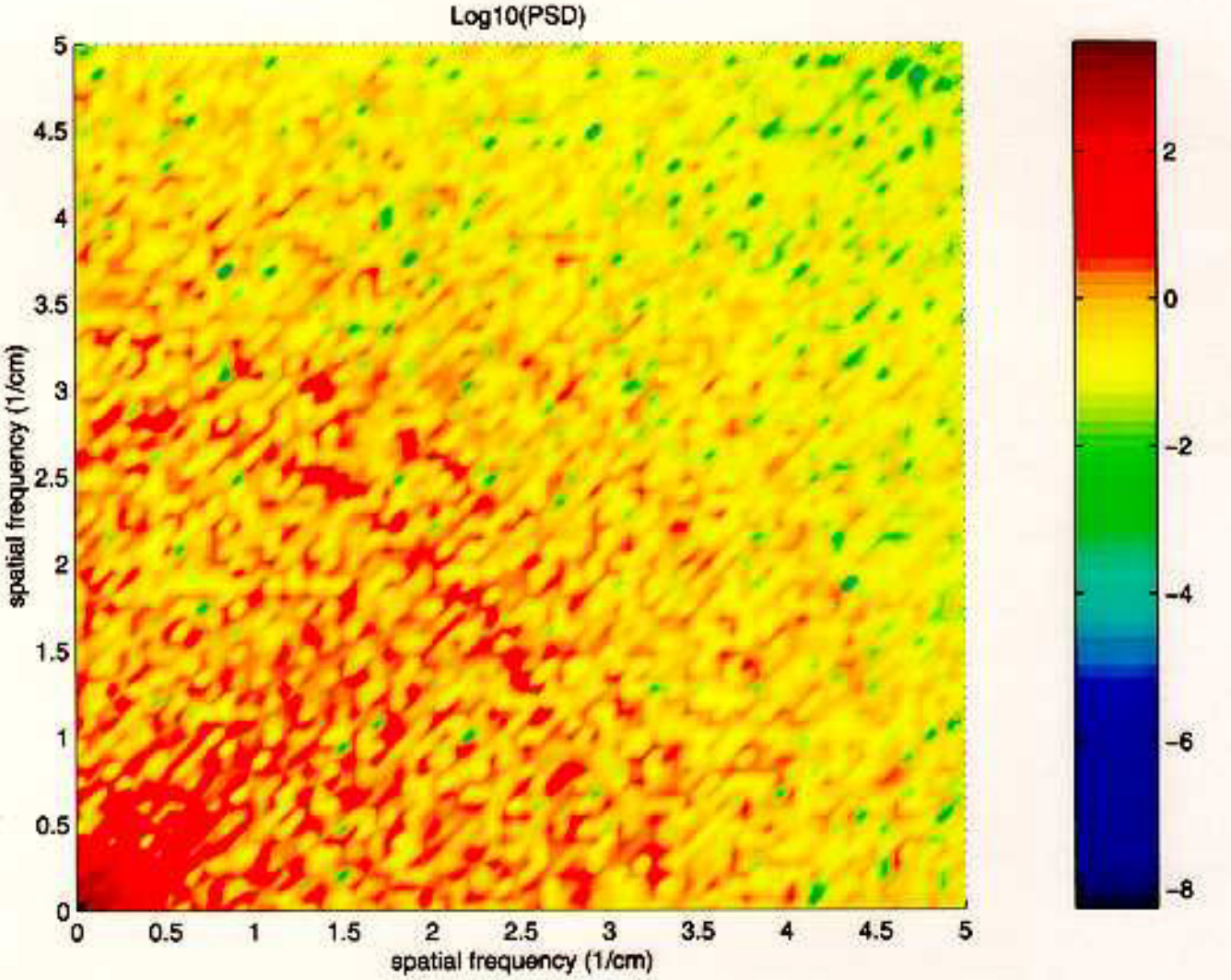
Log10(PSD)
spatial frequency (1/cm)
spatial frequency (1/cm)
0
0.5
1
1.5
2
2.5
3
3.5
4
4.5
5
2
0
−2
−4
−6
−8

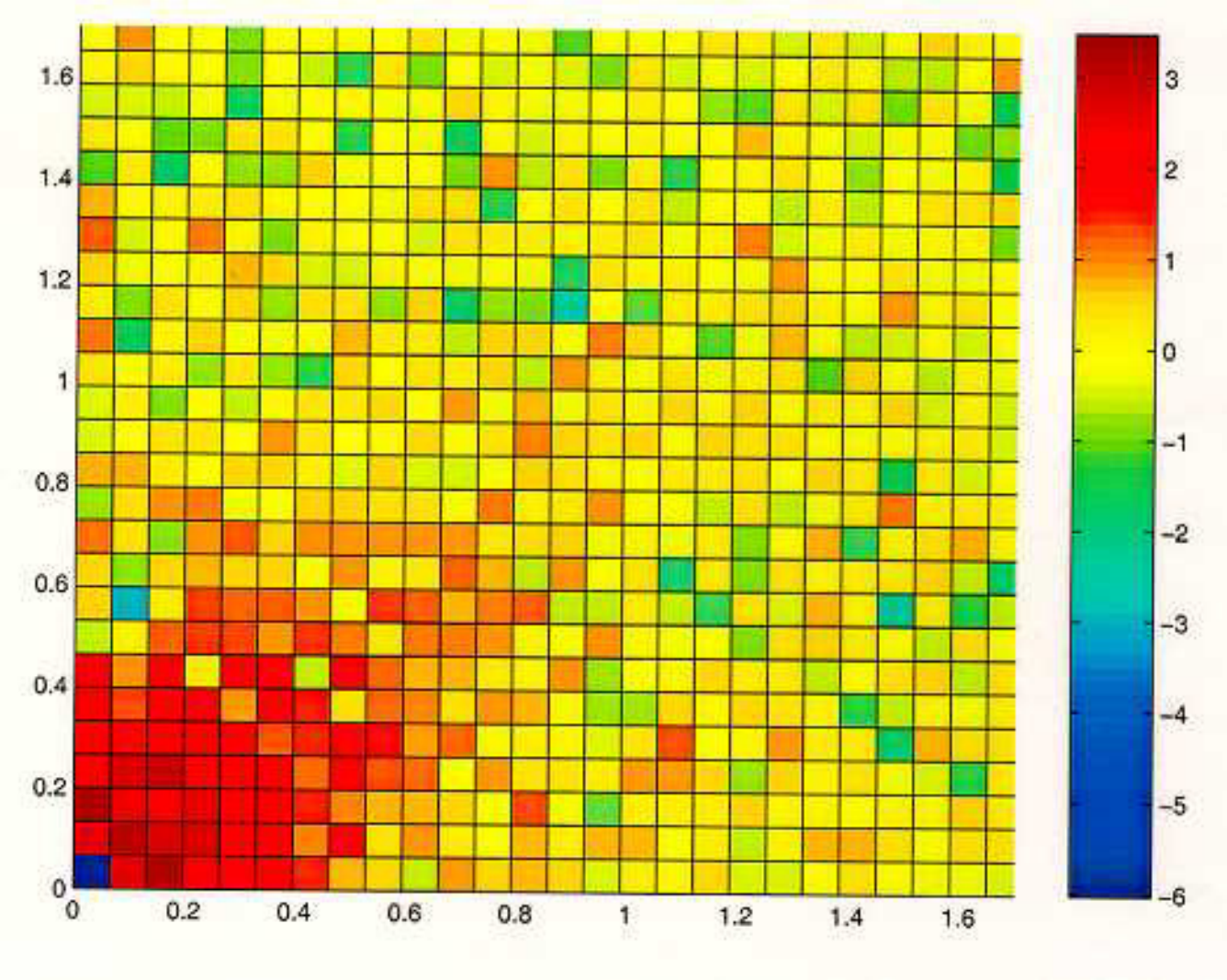
1.6
1.4
1.2
1
0.8
0.6
0.4
0.2
0
0
0.2
0.4
0.6
0.8
1
1.2
1.4
1.6
3
2
1
0
−1
−2
−3
−4
−5
−6

Data extrapolation beyond the measured area

- linear interpolation in the Fourier transform domain
- linear interpolation in the Fourier transform with phase randomization
- radial specular reflections of patterns

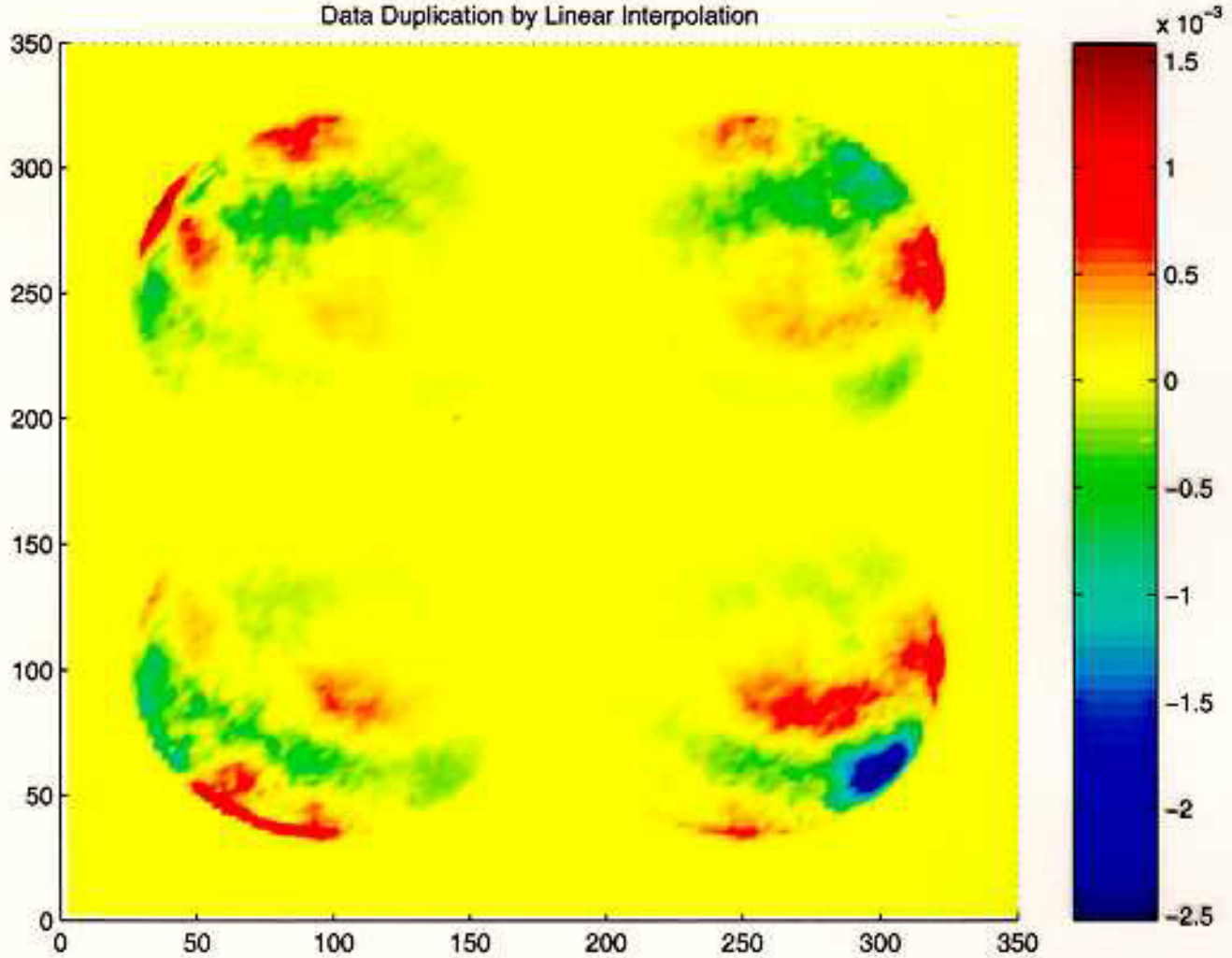
Data Duplication by Linear Interpolation
x 10^-3
1.5
1
0.5
0
-0.5
-1
-1.5
-2
-2.5
350
300
250
200
150
100
50
0
0
50
100
150
200
250
300
350

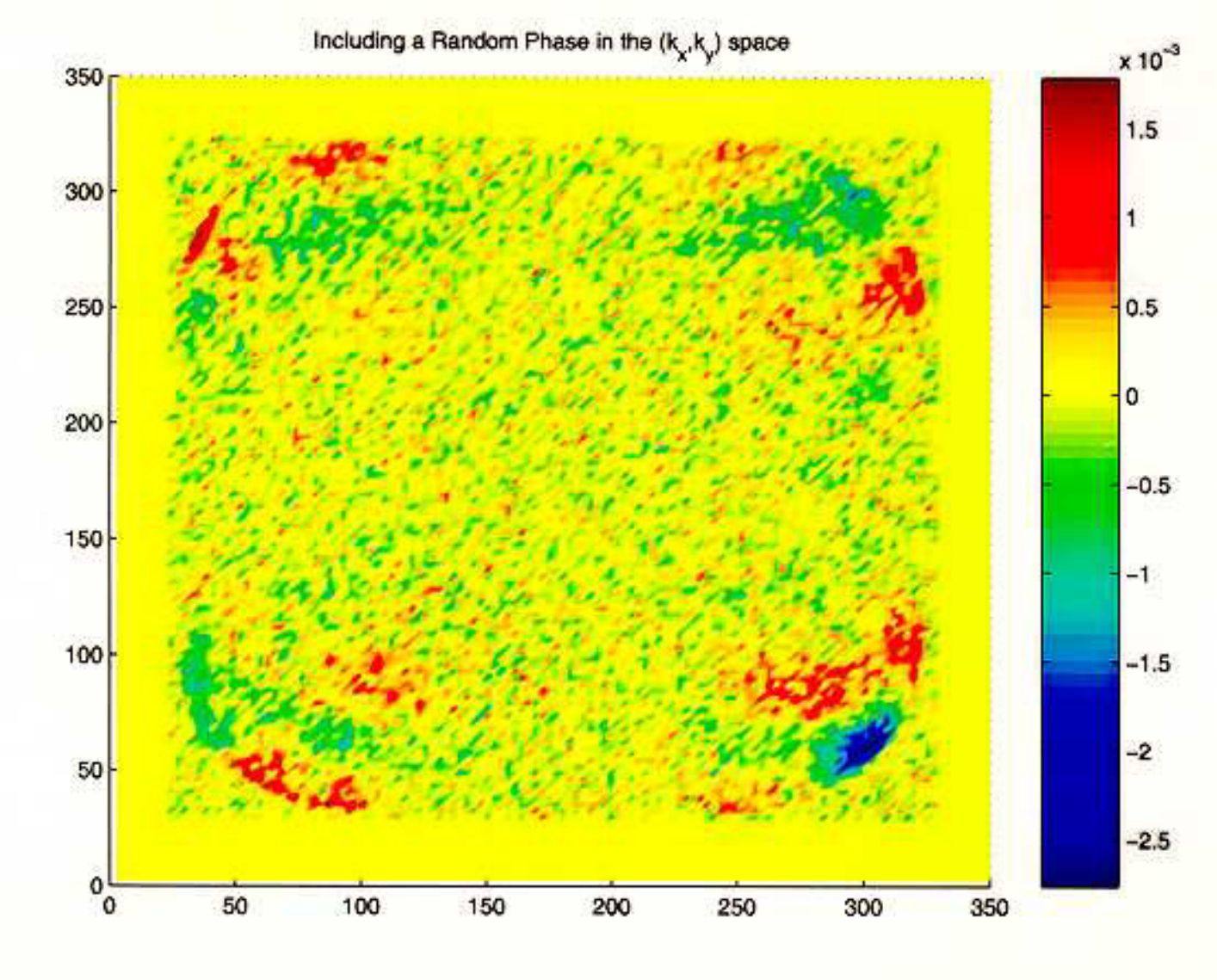
Including a Random Phase in the (k_x,k_y) space
x 10^-3
1.5
1
0.5
0
-0.5
-1
-1.5
-2
-2.5
350
300
250
200
150
100
50
0
0
50
100
150
200
250
300
350

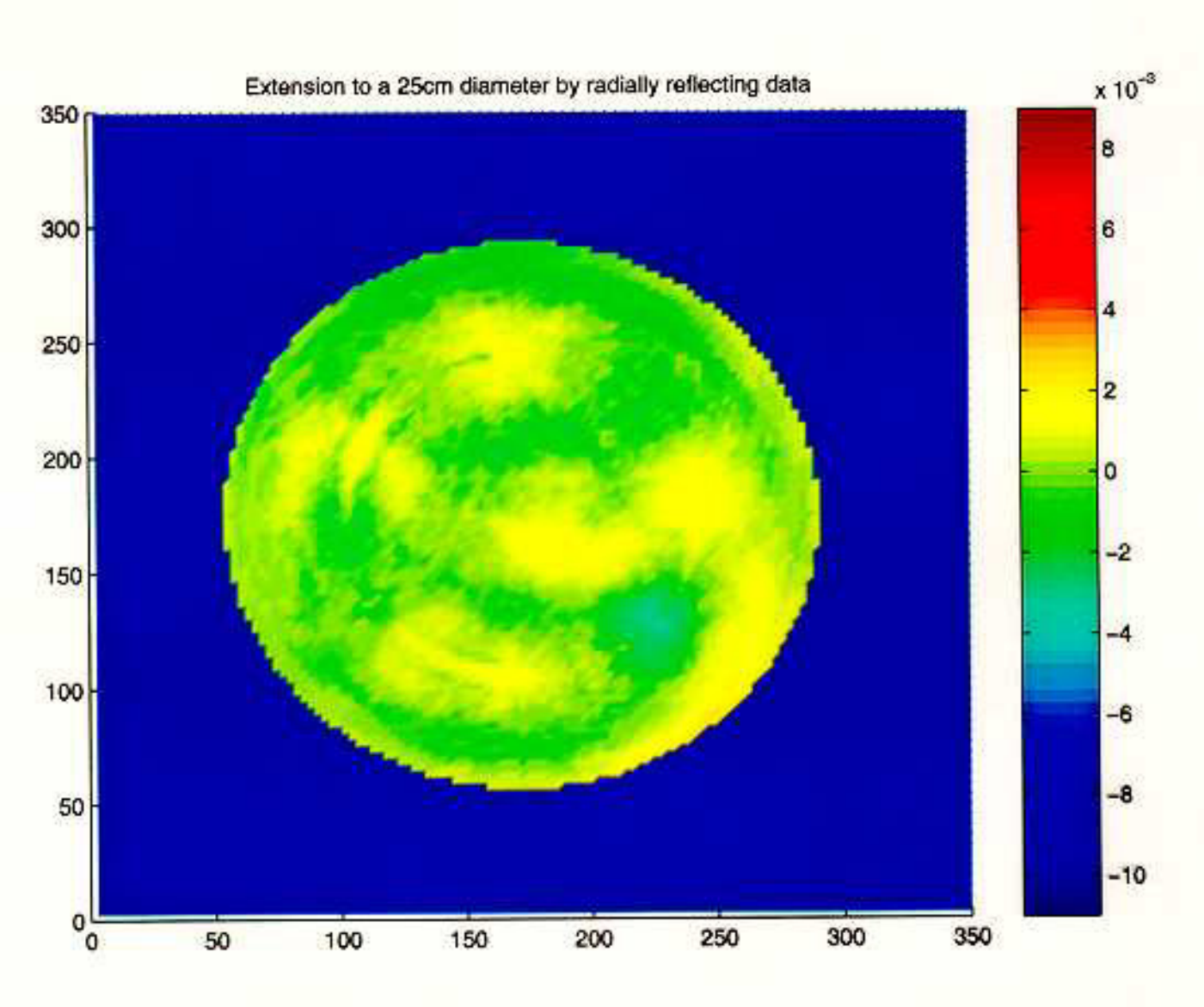
Extension to a 25cm diameter by radially reflecting data
x 10^-3
8
6
4
2
0
-2
-4
-6
-8
-10
350
300
250
200
150
100
50
0
0
50
100
150
200
250
300
350

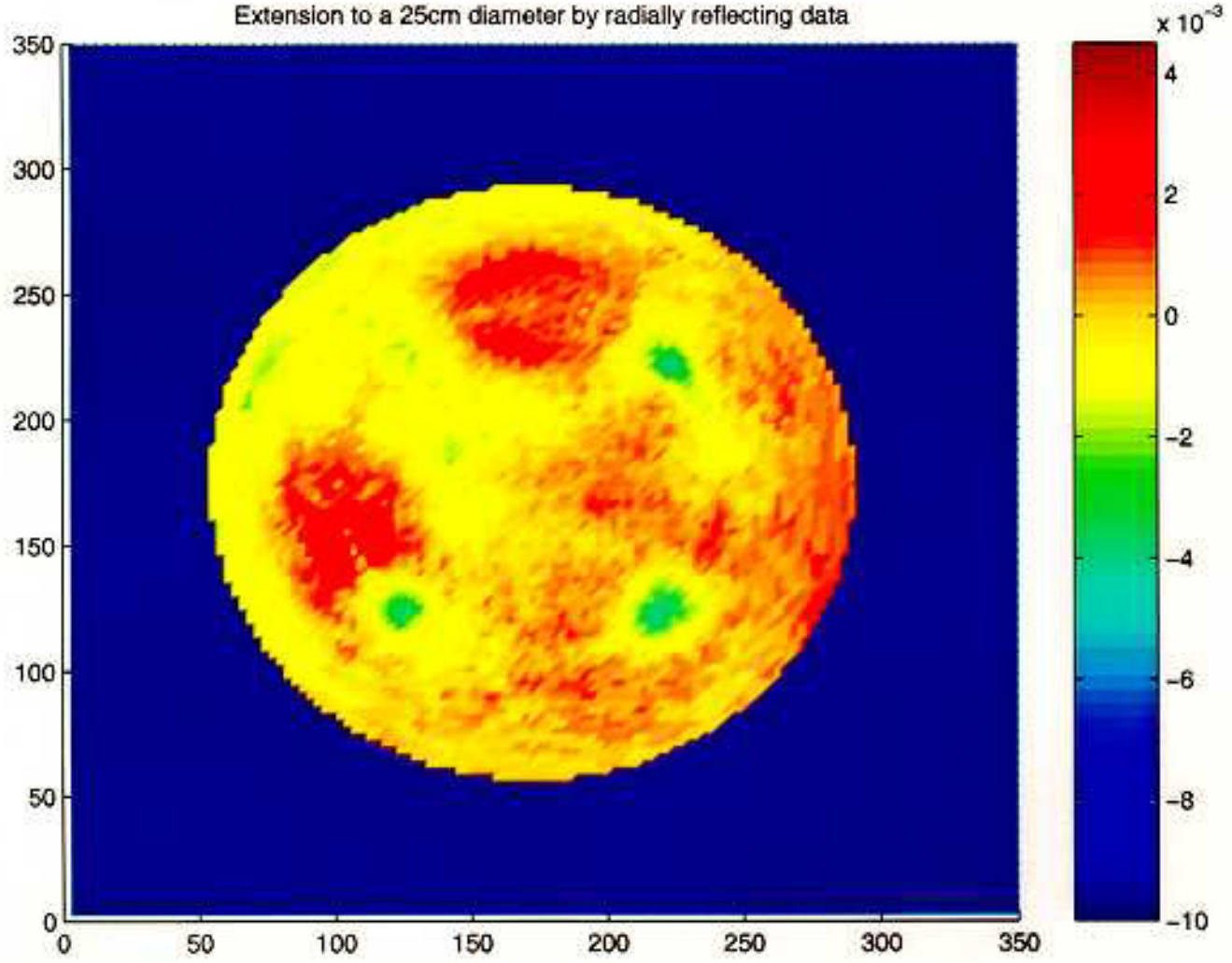
Extension to a 25cm diameter by radially reflecting data
x 10^-3
4
2
0
−2
−4
−6
−8
−10
350
300
250
200
150
100
50
0
0
50
100
150
200
250
300
350

Problem of extending the true data outside the measured area

Dual purpose Can the imperfections on the external region be discarded or do they actually disturb?

Which functions evaluated on the original data are useful/necessary for the extrapolation?

Solution

Computing the correlation functions of the original set of real data. Studying the arrangement in cluster of the imperfections using the Fourier transforms and considering similar occurences for the unknow quantities.

Non trivial mathematical procedure

In the time domain this is the same problem of reconstructing a signal.

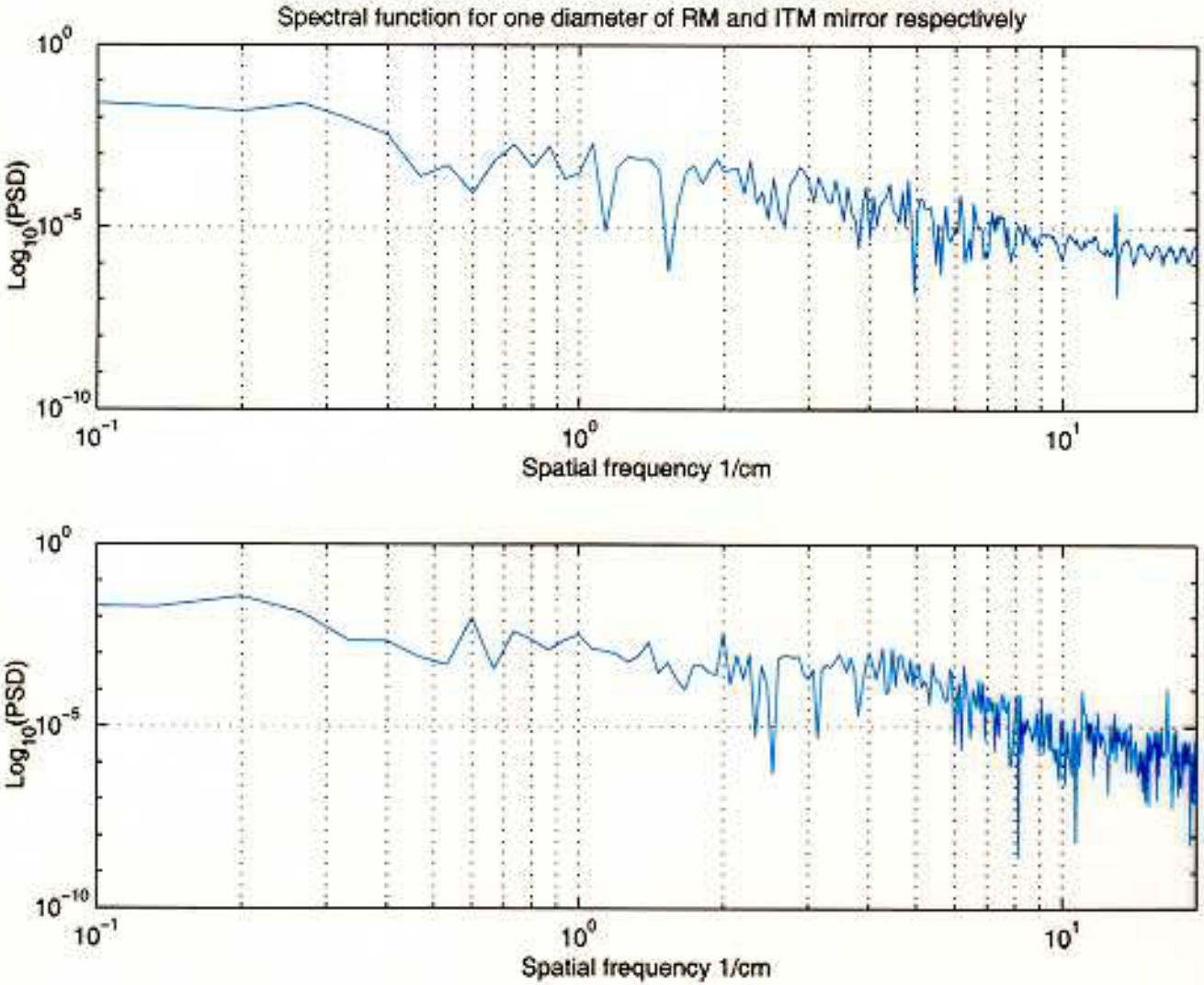
Spectral function for one diameter of RM and ITM mirror respectively
10^0
10^{-5}
10^{-10}
$\mathrm{Log}_{10}(\mathrm{PSD})$
10^{-1}
10^0
10^1
Spatial frequency 1/cm
10^0
10^{-5}
10^{-10}
$\mathrm{Log}_{10}(\mathrm{PSD})$
10^{-1}
10^0
10^1
Spatial frequency 1/cm

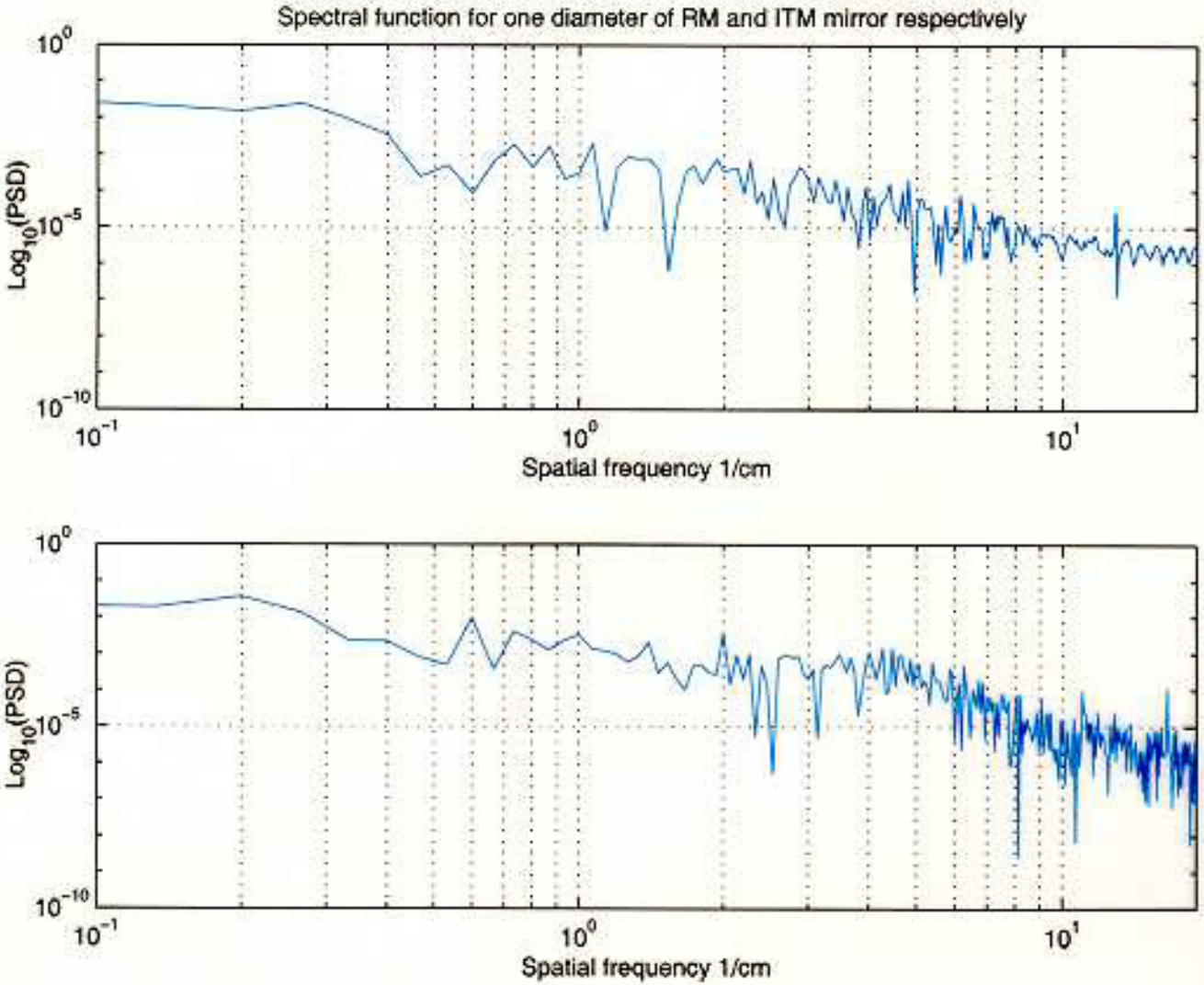
Spectral function for one diameter of RM and ITM mirror respectively
10^0
10^{-5}
10^{-10}
$\mathrm{Log}_{10}(\mathrm{PSD})$
10^{-1}
10^0
10^1
Spatial frequency 1/cm
10^0
10^{-5}
10^{-10}
$\mathrm{Log}_{10}(\mathrm{PSD})$
10^{-1}
10^0
10^1
Spatial frequency 1/cm

Future Project

Studies will address every aspects which can be related to the interaction with simulated interferometer dynamics.

---

1. Effects on beam
   using measured mirrors & uniform value for the extension on the anulus

2. Effects of arbitrary perturbations on the external anulus checking if different guesses result in different output data from the run

3. Effect of high segmentation in order to recover high frequency modulation correlation (increased computing time is needed)

4. Implementation into simulation of all the optical dynamics.